Controlled heat flux measurement across a closing nanoscale gap and its comparison to theory

Y. Ma, A. Ghafari, B. Budaev and D. Bogy*

Computer Mechanics Lab, University of California, Berkeley, CA, 94720, USA

Abstract

We present here a controlled measurement of heat flux across a closing gap that is initially less than 10 nm wide between two solid surfaces at different temperatures. The measured heat transfer is compared with our published theoretical analyses of this phenomenon that show thermal radiation dominates the heat transfer for gaps wider than about 1-2 nm, but phonon conduction dominates between 1-2 nm and contact. The experiments employ a thermal actuator (TA) mounted on a rocking base block for coarse positioning that supplies Joule heating to an embedded element to cause thermal expansion of a localized region for less than 10 nm spacing control, together with an embedded near-surface resistive thermal sensor (TS) to measure its temperature change due to the heat flux across the gap. The measured results are in general agreement with the theoretical predictions, and they also agree with common sense expectations. This paper not only shows nanoscale heat transfer measurement across a closing gap, it also lends additional strong support to the validity of the referenced theoretical developments.

Many applications in nanotechnology require the understanding of heat transfer across nanoscale gaps between two bodies at different temperatures[1]. In connection with the emerging data storage technology called Heat Assisted Magnetic Recording (HAMR) we have undertaken over the last decade both theoretical and experimental studies in nanoscale heat transfer.

As discussed in our recent papers [2-4] classical methods[5] of calculating heat transfer are not valid at the nanoscale, because the underlying theories do not hold for nanoscale dimensions. The theory in [3, 4], which is based on the wave character of both thermal radiation and phonon thermal conduction, has been shown to satisfy all known requirements for heat transfer across a closing gap as opposed to other presented theories[6-8], and it also is in agreement with such observed phenomena as Kapitsa resistance [9] of interfaces and the asymmetric phenomenon known as "thermal rectification".

In order to further test the validity of the published theories in [3, 4] we sought an experiment for measuring heat flux across a gap between two bodies as the spacing between them closes in a controlled manner from 10nm down to contact. Such a controlled experiment is notoriously difficult. Previous experimentalists have been able to make measurements down to 20nm [10-13] and a recently published result was able to control the spacing as close as 2 nanometers[14].

After our attempts to design the experiment using some kind of MEMS actuator and sensor we realized that we already had several such suitable devices in the laboratory. Probably every laboratory has them, and if not they can be purchased in an electronics store for no more than about ten dollars each. They are, indeed, the read-write head sliders in current technology hard disk drives (HDD). Drives containing a half dozen systems like those we used can be purchased for less than one hundred dollars. An

example of such a slider mounted on its suspension and showing its wiring harness is shown in Fig.1

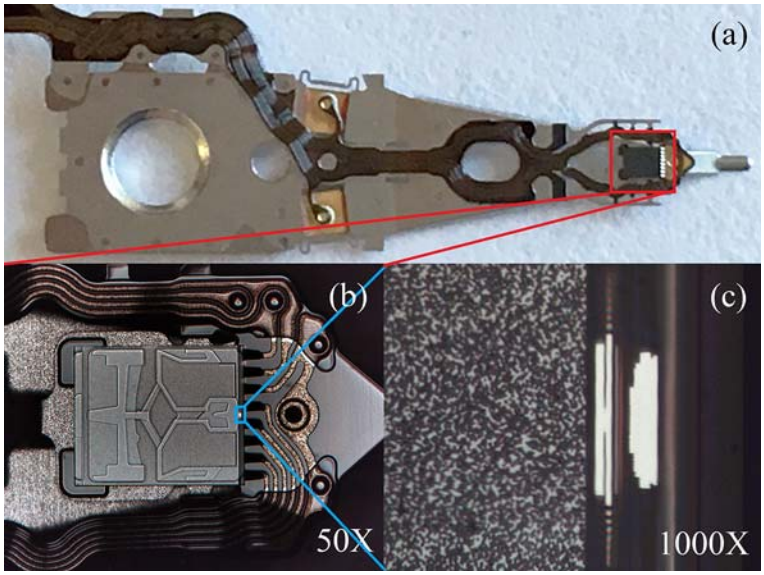

Fig. 1 Under side of a HDD magnetic head and suspension showing: (a) the slider-suspension structure, (b) the slider's air bearing design pattern, its suspension mounting and its wire harness that connects to the various transducers. The black rectangle is the air bearing slider (that carries the head transducers) with dimensions of about 820x700x230 microns. Its material is Al_2O_3-TiC. (c) is a zoom in of the right 20 microns that carries the read-write transducers. The reader with shields is the left white portion; the writer is the right white portion. The speckled material on the left is the slider body material Al_2O_3-TiC. The transducers are embedded in Al_2O_3 and are made of such metals as Fe, Ni, Cu, and Cr.

Embedded in the end structure of Fig. 1c is also a resistive heating element, we call a thermal actuator (TA), placed near and a few microns above the write transducer, and between the read and write transducers nearer to the surface is a very small resistive

temperature sensor (TS). All of these transducers and sensors are connected to the wire harness shown in Figs. 1 a, b, and they can be connected to various electronic instruments for measurements and control. In magnetic recording the TA can be used to supply heat to the region above the transducers and cause them to protrude toward the disk for controlling the spacing between the transducers and the magnetic disk. We make use of these TA and TS features to control the spacing and measure the heat flux in our experiments.

In the present paper we first apply this new theory [2-4] to the stack of material layers and gap H to show how the heat transfer coefficient based on both radiation and phonon conduction depends on the nanoscale spacing gap down to and including contact. Graphical solutions are presented for the calculated interface structure used in the experiments.

Next we perform a series of experiments on a silicon wafer using the TS device to observe the temperature change of the interfaces during the process of closing the gap by supplying power to the TA. The experimental observations are compared with the theoretical calculations, and general agreement between them is obtained.

1. Calculation of the heat transfer coefficient between the two surfaces at different temperatures.

Consider the simple material-gap interface structure shown in Fig 2. In this calculation we use Al_2O_3 for halfspace A, representing the hotter embedding material of the TS, and Si for halfspace B, representing the cooler Si wafer.

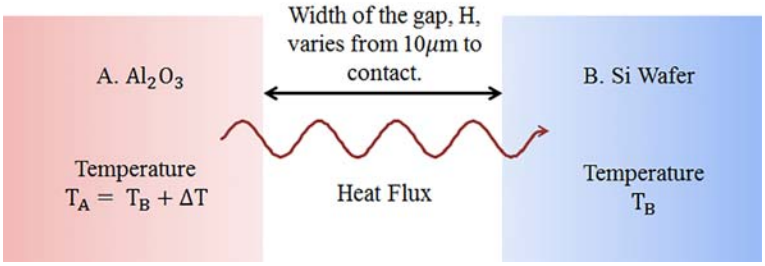

Fig. 2 Structure of the material-gap interface

We assume the temperatures are different in the two sides and calculate the heat flux across the gap. According to the theory in [3, 4] we need to calculate both the radiation and phonon conduction contributions. The radiation heat transfer is based on EM waves. The distribution of energy transferred is determined by an extension of the Planck law to non-equilibrium systems that have a net heat flux. The reflection coefficient R can be calculated for any layered structure by known means. The radiation heat flux is governed by the equation [4]

$$Q(T_A, T_B) = N \int_0^{\omega_D} \int_0^{\theta_A^*} \left\{ (1 - |R(\omega,\theta)|^2) \left[P\left(\omega, \theta; T_A, \frac{Q}{Q_A}\right) - P\left(\omega, \theta; T_B, -\frac{Q}{Q_B}\right) \right] \right.$$
$$\left. - 2|R_A(\omega,\theta)|\sqrt{1 - |R(\omega,\theta)|^2} P_{AB}(\omega, \theta; T_A, T_B, Q) \cos\chi \right\} d\Omega$$

where Q is the heat flux, N is the number of polarizations, R is the reflection coefficient, P is the distribution of emitted energy as a function of angle and frequency of the waves, and χ is a random phase shift. A similar equation holds for phonon conduction, as shown in [4]. For the structure considered here R is sufficiently small that we can ignore

the last term in the calculations. Using this approach we calculated the total heat flux for the above structure for various temperature differences between the two sides. The heat transfer coefficient is defined here as $h=Q/\Delta T$.

The results for the system depicted in Fig. 2 are plotted in Fig. 3. It shows that for H greater than about 10^4 nm the classical Stefan-Boltzmann result is obtained. Between 10^4 and 10^2 nm the radiation heat transfer is no longer predicted by the classical result, but instead increases by about two orders of magnitude. As the gap reduces below 10^2 nm the radiation heat transfer coefficient remains constant down to contact, but as H is reduced to between 1 and 2 nm the phonon conduction comes into play and the heat transfer coefficient rapidly increases with further reduction of H. The three curves represent the calculations for different temperature differentials, and while the values of h are slightly different, the overall dependences on the gap H of the heat transfer coefficients are almost the same. This result shows a tremendous increase in the heat transfer coefficient, more than seven orders of magnitude, over the last 1 nm before contact, due to phonon conduction.

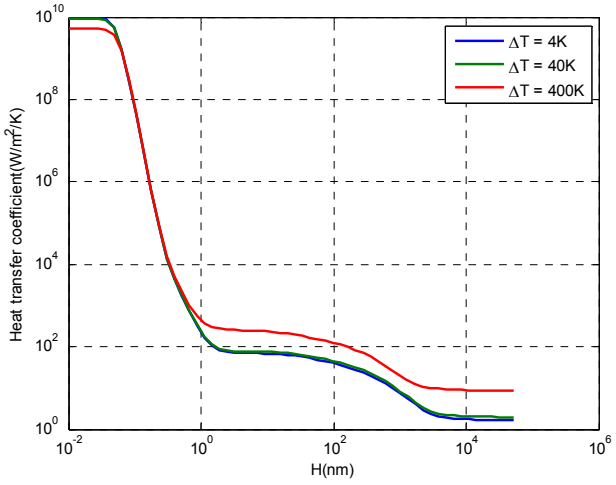

Fig. 3 Total heat transfer coefficient ($Q/\Delta T$) from both radiation and phonon conduction as a function of the gap width H for various temperature differences.

2. TA-TS system setup

A side view sketch (not to scale) of the experimental system is shown in Fig. 4. As depicted there, in the experiments the TA is used to cause thermal expansion of a localized region for nanoscale spacing control, and the TS is used to measure its temperature change due to the heat flux across the gap that occurs because of a temperature differential between the hotter TS and the opposing plate. The slider block has a designed and fabricated crown of about 7 nm on its surface that opposes the plate. This crown together with the suspension connection and the TA are critical for control of the gap.

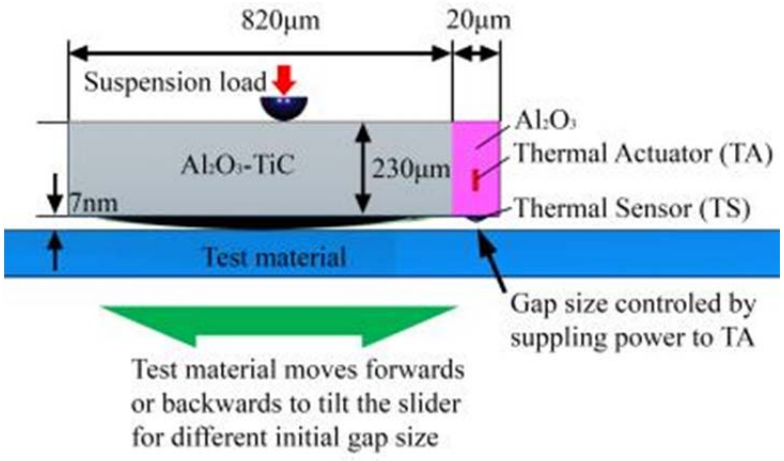

Fig. 4 Thermal actuator TA and thermal sensor TS attached to one end of a rigid block having a 7 nm crown.

During operation the heater of the TA in Fig. 4 raises the temperature in the structure that contains the resistive sensor element TS. This temperature increase causes a thermal expansion (bulge) that results in a spacing reduction between these elements and the surface on which the block is placed. The block can be rocked back and forth on its crown by use of a micrometer stage to move the wafer and thereby achieve a coarse adjustment of the initial spacing between the TS and the test surface.

These actuators have been extensively studied by modeling and experimentation[15]. In a typical TA controlled protrusion region profile, the area less than 1 nm from the peak is about 5 microns across, and therefore it can be regarded as a half space. Or stated another way a lateral span of roughly 70,000 nm has an elevation change of about 12 nm.

In these experiments we use a Si wafer for the contacting plate element because of its smooth surface and known thermal properties. The method can also be used with other reasonably smooth materials to measure their spatial variations in heat transfer coefficients, which will be demonstrated in a future paper.

3. Experimental measurement of heat flux across a nanoscale gap

The control of this experiment is extremely delicate, and it requires special instrumentation and skilled manipulation by the experimentalist. This capability has been developed over several years of work with these systems in the Computer Mechanics Laboratory at UC Berkeley.

Fig. 5a shows several experimental results. The top curve is the free space heating result for the case when the Si wafer is not present. It shows the rate at which heat is lost to the surroundings when the TS is spaced at a distance sufficiently far from the wafer.

The next lower curves represent TA heating experiments for different initial separations between the TS and the Si wafer. The top most of these curves corresponds to a case where the initial separation was about 10-12 nm (the system has been calibrated and it has been found that 10 mW of TA power corresponds to about 1 nm of bulge when no heat sinks are near). The curves below it correspond to results for smaller initial separations. As can be seen, all of the curves initially show a linear increase of TS temperature with an increase of TA applied power. (label the left graph a. and the right graph b. Put a dashed rectangle around the part of a that is shown in b)

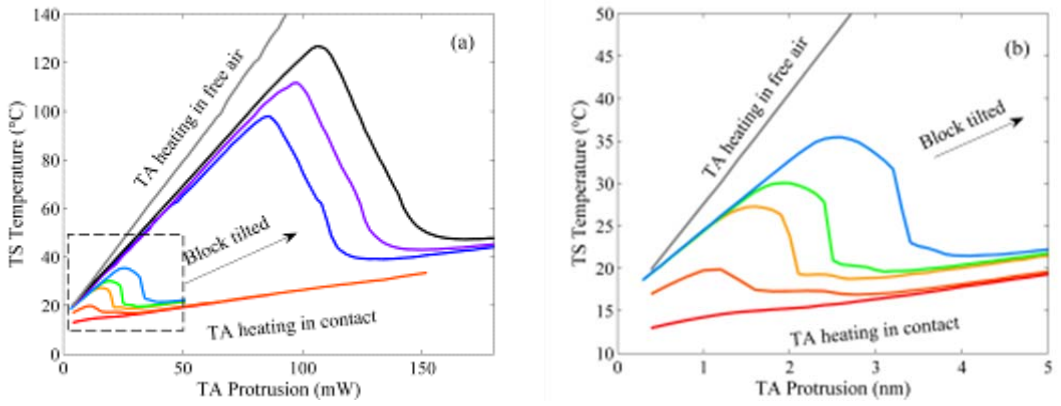

Fig. 5 a) TS temperature change vs TA power for the block resting on the wafer as shown in Fig.4. The block's tilt can be adjusted on its crown by a micrometer system so that the initial spacing between the TS and the wafer is only a few nm. b) Close initially spaced results in a) plotted as TS vs TA protrusion

In all of the curves in Figs. 5a, the TS signal reaches a maximum and then reduces to a minimum before again increasing linearly with TA power. The rate of TS increase with TA power in the lower region is determined by the rate of increase of temperature when the TS is in contact with the Si wafer. The amount of TA power required for the TS to reach a peak depends on the initial gap that is controlled by the initial positioning of the Si wafer by use of the micrometer stage. For the higher power results (larger initial spacing) it appears that a difference of about 40 mW of TA power is required to span the gap between the maximum and minimum TS temperatures. However, it is likely that the free-space rate of 10 mW per nm protrusion change does not hold as the TS approaches the cooler Si wafer. We assume that the protrusion is proportional to the TS temperature and the temperature is proportional to the TA power, so that

$$H = H_0 - aP$$

But as the TS begins to lose heat to the Si wafer the temperature becomes a nonlinear function of P and the relationship becomes

$$H = H_0 - aP + k(P-P_0)^2 + \ldots$$

In order to understand the process better we studied the lower power sequence of curves in Fig. 5a. Using the 10 mW per nm calibration we converted these results to TS Temperature change vs TA protrusion in nm as shown in Fig. 5b.

The shapes of the curves in Fig. 5b are similar in that they all show about the same 1 nm of protrusion between their maxima and minima. They can be explained by referring to the theoretical calculations shown in Fig. 3, where it is seen that phonon conduction

begins to increase the heat transfer coefficient around a gap of 1-2 nm, and as the gap closes from there the coefficient increases by several orders of magnitude. This accounts for the initial smooth fall off of the TS vs protrusion curves in Fig 5b followed by the rapid decrease in TS temperature until the contact condition is reached.

Still, there remains some question as to where contact occurs in the experimental results shown in Figs. 5a and 5b. Indeed, there is a fundamental question about contact. We assume that contact does not mean that atoms of one surface touch atoms of the other surface, or that they are chemically connected to molecules or a crystalline structure. We understand that reaching contact is a continuous process, which starts when the surfaces become affected by intermolecular forces acting across a gap, and ends when a further increase of the pressure causes a disproportionally smaller effect on the observed properties of the structure. Because all of the curves in Figs. 5a and 5b drop to the same line that shows a linear increase with continued increase in TA power, it is reasonable to conclude that this linear line represents the rate at which the TA can increase the temperature of the TS when the latter is in contact with the Si wafer.

Another series of experiments, called here "load-unload" experiments was conducted to shed more light on this contact question. In these experiments the TA power was increased to a certain value and then it was decreased. The results are displayed in Fig. 6 where the initial starting position was only about 3 nm from the Si wafer. As shown in Fig. 6 the TS temperature increased and decreased along the same line as the TA protrusion was increased up to about 3.2 nm. If however, the TA protrusion was

increased slightly more to about 3.5 nm there occurred a hysteresis loop in the load-unload curve. This loop was more pronounced if the maximum TA protrusion was about 3.7 nm, and substantially more pronounced if the TA protrusion reached 4 nm. Finally, when the TA protrusion reached 4.2 nm the unload curve first traversed a short segment of the linear contact curve of Fig. 6 in its unload path. It is remarkable that these experiments are repeatable, and show distinct differences when one realizes that the protrusion differences are only about 0.2 nm between them. We conclude from this series of experiments that the lower linear TS temperature versus TA protrusion envelope curve defines the contact conditions for the sequence of experimental results shown in Fig 6.

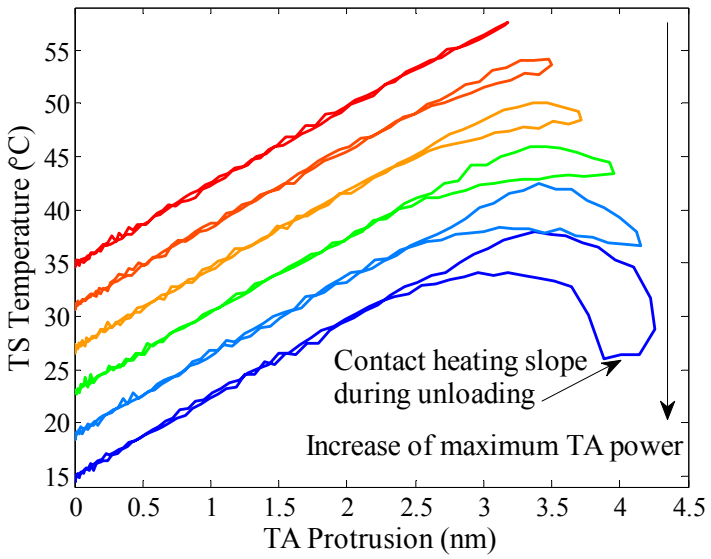

Fig. 6 Load-unload experiments showing the onset of contact, the TS temperature labels are for the bottom curve. The other curves are uniformly shifted up

4. Explanation of the experimental results according to the theory

First it should be noted from Fig. 3 that the theoretical calculation shows for gaps between 80 nm and 2 nm the heat transfer is all due to radiation and it is essentially independent of the spacing in this range. For spacings below about 1-2 nm the flux begins to increase rapidly as H decreases, climbing by as much as 7 orders of magnitude until reaching the contact value when H reaches the atomic spacing range. This calculated result is consistent with the experimental observations. First the free air result in Fig. 5a has as initial slope greater than the initial slopes of the less than10 nm initially spaced results. These slopes are consistent with the constant h values of radiation heat transfer in the 2 – 80 nm range in Fig. 3. The initial slopes of the less than 3 nm initial gap curves in Fig. 5a, b are somewhat lower and begin to bend down, at first gradually, similar to the increase of h in Fig. 3 for H less than 2 nm, and then when H reaches about 1 nm the curves in Fig. 5a,b drop rapidly indicating the phonon conduction heat transfer as shown in that spacing range in Fig. 3.

5. Conclusions

The measurement results presented here for the heat transfer between two bodies at different temperatures as the nanoscale gap between them closes to contact are in general agreement with the theoretical predictions of the wave based theory for radiation and phonon conduction.

To the best of our knowledge this is the first experimental observation of heat transfer across a closing nanoscale gap between bodies at different temperatures in which the

spacing is controlled in the nanoscale range down to less than one nanometer and into contact. And the measured results compare well with the first theoretical development that can explain the experiments without some ad hoc adjustments for each individual case.

Acknowledgement

This work was supported by the Computer Mechanics Laboratory and the Mechanical Engineering Sciences Graduate Fellowship fund at the UC Berkeley.

References

1. Kryder, M. H., et al. Heat assisted magnetic recording. *Proc IEEE* **96,** 1810-1835 (2008).

2. Budaev, B. V. & Bogy, D. B. Extension of Planck's law of thermal radiation to systems with a steady heat flux. *Annalen der Physik* **523,** 791-804 (2011).

3. Budaev, B. V. & Bogy, D. B. Computation of radiative heat transport across a nanoscale vacuum gap. *Appl.Phys.Lett.* **104,** 061109 (2014).

4. Budaev, B. V. & Bogy, D. B. Heat transport by phonon tunneling across layered structures used in heat assisted magnetic recording. *J.Appl.Phys.* **117,** 104512 (2015).

5 Planck, M. *The theory of heat radiation* (P. Blakiston's Son & Co., 1914).

6. Rytov, S. M. *Theory of electrical fluctuations and thermal radiation* (Air Force Cambridge Research Center, Bedford, MA, 1959).

7. Rytov, S. M., Kravtsov, Yu. A. & Tatarskii, V. Elements of random fields. *Principles of Statistical Radiophysics* **vol 3,** (1989).

8. Polder, D. & van Hove, M. Theory of radiative heat transfer between closely spaced bodies. *Physical Review B* **4,** 3303 (1971).

9. Kapitsa, P.L. The study of heat transfer in helium II. *J.Phys.(USSR)* **4,** 181-210 (1941).

10. Shen, S., Narayanaswamy, A. & Chen, G. Surface phonon polaritons mediated energy transfer between nanoscale gaps. *Nano letters* **9,** 2909-2913 (2009).

11. Rousseau, E., et al. Radiative heat transfer at the nanoscale. *Nature Photonics* **3,** 514-517 (2009).

12. Song, B., Fiorino, A., Meyhofer, E. & Reddy, P. Near-field radiative thermal transport: From theory to experiment. *AIP Advances* **5,** 053503 (2015).

13. Song, B., et al. Enhancement of near-field radiative heat transfer using polar dielectric thin films. *Nature nanotechnology* **10,** 253-258 (2015).

14. Kim, K., et al. Radiative heat transfer in the extreme near field. *Nature* (2015).

15 Zheng, J. Dynamics and stability of thermal flying-height control sliders in hard disk drives. (2012).